Cooperativity and Specificity of Association of a Designed Transmembrane Peptide

Holly Gratkowski, Qing-hong Dai, A. Joshua Wand, William F. DeGrado, and James D. Lear
The Johnson Research foundation, Department of Biochemistry and University of Pennsylvania, Philadelphia PA 19104-6059 USA

ABSTRACT Thermodynamics studies aimed at quantitatively characterizing free energy effects of amino acid substitutions are not restricted to two state systems, but do require knowing the number of states involved in the equilibrium under consideration. Using analytical ultracentrifugation and NMR methods, we show here that a membrane-soluble peptide, MS1, designed by modifying the sequence of the water-soluble coiled-coil GCN4-P1, exhibits a reversible monomer-dimer-trimer association in detergent micelles with a greater degree of cooperativity in C14-betaine than in dodecyl phosphocholine detergents.

INTRODUCTION

Extensive information is available on the thermodynamics of folding of many water-soluble proteins. This has been facilitated not only by the large database of water-soluble protein structures, but also by the fact that many water-soluble proteins exhibit reversible, apparent two-state folding, which simplifies thermodynamic analyses. Although there has been promising progress recently in developing reversible folding systems for thermodynamics studies of membrane proteins (Chen and Gouaux, 1999; Fisher et al., 1999; Fleming et al., 1997; Fleming and Engelman, 2001; Gratkowski et al., 2001; Zhou et al., 2001), in general methods have not been developed in which native membrane proteins reversibly denature in a two-state manner. Additionally, there is the need to consider the properties of the detergents or lipids in the thermodynamic analysis of a membrane protein system (for a review, see Garavito and Ferguson-Miller, 2001). For example, dimerization of the transmembrane segment of glycophorin is less tight and equilibrates much faster in sodium dodecyl sulfate (SDS) than in zwitterionic detergents (Fisher et al., 1999).

Water-soluble coiled coils have been invaluable in developing an understanding of the thermodynamics of protein folding. For example, derivatives of the coiled-coil peptide GCN4-P1 have been shown to be in an equilibrium among monomers, dimers, and trimers, with the predominant species switching in response to single amino acid changes, the binding of small molecules, and temperature (Gonzalez et al., 1996a, 1996b, 1996c). Additionally, during the early years of protein design studies, a family of designed coiled-coil peptides was shown to exist in a noncooperative monomer-dimer-trimer equilibrium (Betz et al., 1995). Design refinements led to a peptide with a highly cooperative monomer-trimer equilibrium (Boice et al., 1996).

Using a strategy similar to that used in the study of water-soluble model peptides, it has been found that model membrane peptides, normally insoluble in aqueous solutions, can be conveniently studied in detergent micelles. Membrane proteins such as the glycophorin dimer (Lemmon et al., 1991) and the influenza virus M2 tetramer (Sakaguchi et al., 1997) appear to form a single oligomeric state. However, phospholamban, another well-studied membrane protein (Arkin et al., 1997; Cornea et al., 1997; Li et al., 1999), which appears to function (as a Ca^{2+} −ATPase inhibitor) *in vivo* as a monomer, forms association states ranging from dimers to pentamers. To understand the forces specifying particular aggregation states, the water-soluble GCN4-P1 peptide would appear to be an ideal system for study if converted into a membrane-soluble form. Thus, in independent studies, the exterior of GCN4-P1 was mutated to hydrophobic residues while the interior residues remained untouched (Choma et al., 2000; Zhou et al., 2000). Choma *et al.* used SDS-PAGE (polyacrylamide gel electrophoresis), analytical ultracentrifugation, and fluorescence resonance energy transfer methods to show that their peptide, denoted MS1, formed trimers. Quantitative analysis of the analytical ultracentrifugation (AUC) data showed a relatively cooperative monomer-trimer equilibrium in the detergent C14-betaine but the data were insufficient to accurately determine the extent of intermediate dimer formation. Using SDS-PAGE, Zhou *et al.* reported a dimer for their membrane-solubilized GCN4 peptide fused to the water-soluble protein staph nuclease. However, a mixture of monomers, dimers, and trimers was observed when the peptide portion alone was mixed with the fusion protein, indicating a lack of specificity of the peptide oligomerization. Interestingly, in SDS-PAGE experiments performed by Choma et al., the peptide migrated to a band denoting a single trimeric species. It was unclear whether the differences observed by the two groups were due to the presence of a fusion protein or due to the different levels of cooperativity of the membrane-solubilized GCN4-P1 systems.

To follow the effect of peptide sequence changes on the thermodynamics of association, it is necessary to measure

Submitted January 11, 2002 and accepted for publication May 8, 2002

Address reprint requests to James D. Lear, The Johnson Foundation, School of Medicine, 36th and Hamilton Walk, Philadelphia, PA 19104-6059. Tel.: 215-898-2071; Fax: 215-573-7229; E-mail: lear@mail.med.upenn.edu.

0006-3495/02/09/1613/07 $2.00

the equilibrium dissociation constants of all relevant aggregation states. Quantitative measurements of equilibrium constants by analytical ultracentrifugation in density-matched detergent micelles have been reported for glycophorin peptides fused to the water-soluble protein, staphylococcal nuclease (Fleming et al., 1997; Fleming and Engelman, 2001). However, the accurate measurement of multistate equilibrium constants of small, water-insoluble peptides in detergent micelles by AUC presents an additional challenge. The goal of the present paper is to quantitatively examine the cooperative association equilibrium of the MS1 peptide in detergent micelles. Here, by combining analytical ultracentifugation with NMR methods, we show that the designed membrane-soluble model peptide, MS1, exhibits a rapid, reversible monomer-dimer-trimer association with a level of cooperativity that is sensitive to small changes in the detergent used for solubilization.

MATERIALS AND METHODS

Peptide synthesis and purification

The sequence of MS1 is BQLIAAVLLLIAVNLILLIAVARLRYLVG, where B represents the unnatural amino acid β-alanine. MS1 was synthesized, labeled with 7-nitrobenz-2-oxa-1,3-diazole (NBD), and purified as described in Choma *et al.* (2000). The labeled peptide, $^{15}N_2$ Asn MS1, was synthesized on an ABI-433A peptide synthesizer using 25% dimethylsulfoxide (DMSO) /75% dimethylformamide (DMF) as the solvent. The synthesis proceeded normally up until the point of the Asn side chain. The labeled N-9-fluoroenylmethyloxycaronyl (Fmoc) amino acid, N-Fmoc-asparagine, N-β-trityl-$^{15}N_2$ (Cambridge Isotope Laboratories, Inc., Andover, MA), was manually coupled for [six]~14 h at room temperature with 2.35 equivalents of the labeled Fmoc amino acid. Equimolar amounts of 2-(1H-benzotriazole-1-yl)-1,1,3,3-tetramethyl-uronium-hexafluorophosphate (HBTU) and N-hydroxybenzotriazole hydrate (HOBT) were used along with 6.05 equivalents of diisopropylethylamine (DIEA). After the coupling was complete, the peptide was washed several times with DMF and returned to the ABI-433A peptide synthesizer. The synthesis was allowed to proceed under normal conditions. After final deprotection, the resin was dried under reduced pressure, and the peptide was cleaved from the resin with trifluoroacetic acid (TFA) (50 mg/ml) using 5% water (v/v), and 1% triisopropylsilane (v/v) as scavengers. After two hours at room temperature, the resin was removed by filtering the TFA solution through glass wool, and washing with a threefold excess of TFA. TFA was removed under a gentle nitrogen stream over a concentrated sodium bicarbonate solution. The peptide was precipitated with equal amounts of cold ether and hexane. After washing several times, the peptide was dried under reduced pressure.

$^{15}N_2$ Asn-MS1 was purified by reverse-phase HPLC at 50°C using buffer A (20% isopropanol, 79.9% water, and 0.1% TFA) and buffer B (20% isopropanol, 60% acetonitrile, 9.9% water, and 0.1% TFA) on a C4 preparatory scale column (Grace Vydac, Hesperia, CA). Separation of peaks was performed on a linear gradient at 0.5%/min. The purity of the peptide was checked by analytical reverse-phase HPLC with a linear gradient using buffer A and buffer B. The molecular weight was confirmed by matrix-assisted laser desorption ionization mass spectrometry (MALDI-TOF) (PerSeptive Biosystems, Foster City, CA).

Analytical ultracentrifugation

Sedimentation equilibrium experiments using a Beckman XLI instrument were performed in six chamber epoxy centerpiece cells. Short column length (0.36 cm) experiments were spun at 40, 45, and 48 KRPM. MS1 samples in 8 mM C14-betaine were also spun at higher speeds (50, 55, and 60 KRPM) and with longer column length (0.77 cm) in aluminum centerpieces. Samples were prepared as described previously (Gratkowski et al., 2001). All samples were labeled with NBD for increased absorbance sensitivity. Experiments in C14-betaine were performed at detergent concentrations of 4 mM and 8 mM. D_2O was added to match the density of the solvent to that of the micelle (Tanford and Reynolds, 1976). Density matches were experimentally determined (Kochendoerfer et al., 1999) to be the following for 4 mM C14-betaine samples with 100 mM sodium phosphate: pH 7, 25°C, 13% D_2O; pH 4, 40°C, 14% D_2O, and pH 7, 40°C, 8% D_2O. For 8 mM C14-betaine samples with 100 mM phosphate pH 7, 25°C, the density match was 12.5% D_2O. Density matches for 10 mM dodecyl phosphocholine (DPC) in 100 mM phosphate were found to be the following: pH 4, 25°C, 38% D_2O; pH 7, 25°C, 33.3% D_2O; pH 4, 40°C, 44% D_2O; and pH 7, 40°C, 31% D_2O. For fitting theoretical curves to the data, peptide molecular weights and specific volumes, calculated using the program Sedinterp (Laue et al., 1992) with revised values of amino acid partial specific volumes (Kharakoz, 1997), were adjusted for H-D exchange as described previously (Salom et al., 2000). The following equilibrium scheme with accompanying definitions of equilibrium constants was used:

$$2M \rightleftharpoons D \quad K_{12} = \frac{M^2}{D}$$

$$3M \rightleftharpoons T \quad K_{13} = \frac{M^3}{T}$$

where M, D, and T denote peptide/detergent mole fractions of monomer, dimer, and trimer, respectively, and K_{12} and K_{13} are the equilibrium dissociation constants of dimer and trimer (calculated using mole fraction units, shown previously to be the appropriate unit for this peptide (Lear et al., 2001)). Data, weighted by their standard error of absorbance measurements, were fit using the Levenberg-Marquardt algorithm provided in Igor Pro (Wavemetrics Inc., Oswego OR) with a user-defined function incorporating an equation (see, e.g., Arkin and Lear, 2001; Scott and others 2001)) applicable to sedimentation equilibrium of this reversible three-state model. Goodness-of-fit was assessed qualitatively by the randomness of the residuals rather than by the reduced χ^2 (defined as $\chi^2/(N_p - X)$, N_p = number of points, X = number of fitting parameters) because the residuals were about $5X$ larger than those expected from the absorbance errors alone. We attribute this to positional variations in window absorbance leading to larger errors than those estimated from the repeated measurements at fixed position as implemented in the XLI software. In results reported here, the magnitude of χ^2 is nevertheless used as a convenient quantitative comparison of fit quality between different models applied to the same data.

NMR experiments

$^{15}N_2$-Asn MS1 was solubilized in ethanol, and an absorbance spectrum was taken at 280 nm (ε = 1400) to determine the concentration. Deuterated DPC (D28 from Cambridge Isotope Laboratories, Inc.) was also dissolved in ethanol. Peptide solutions at 200 μM were mixed with the appropriate amount of DPC. Ethanol was removed under reduced pressure, and the samples were solubilized in 92% 100 mM sodium phosphate pH 4.0 and 8% D_2O. A series of two-dimensional ^{15}N-HSQC spectra were recorded on an Inova 600 MHz spectrometer at 40°C. 1024 complex points were recorded in the t_2 dimension (^1H) and 48 complex points in the t_1 dimension (^{15}N). The ^1H carrier frequency was placed at the water resonance (usually 4.69 ppm), and that of ^{15}N was set at 119.00 ppm. The data were processed using Felix98 (Friedrichs et al., 1994), with matrix size 2048 × 1024 ($t_2 \times t_1$). Peak volumes were integrated in Felix98, and the percentage for each was calculated.

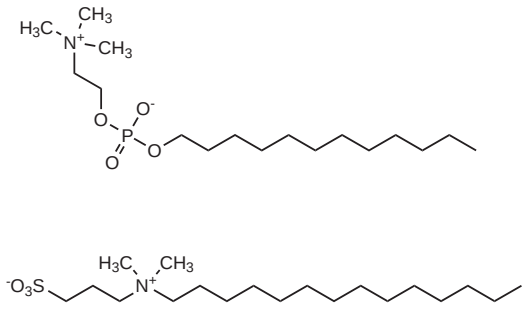

FIGURE 1 Chemical structures of DPC (*top*) and C14-betaine (*bottom*).

RESULTS

Analytical ultracentrifugation

The equilibrium association of the MS1 peptide was determined by sedimentation equilibrium in C14-betaine and DPC micelles (structures shown in Fig. 1). In previous studies in C14-betaine, MS1 appeared to exist primarily as monomers and trimers, but a monomer-dimer-trimer equilibrium model provided a slightly better fit (20% lower χ^2) to the data (Choma et al., 2000). To achieve greater accuracy, MS1 samples were prepared in 8 mM C14-betaine and spun at higher speeds in long-column, aluminum centerpieces. This allows higher volumetric concentrations of peptides to be used and the development of greater concentration gradients and sensitivity of fits to the equilibrium constants. In Fig. 2 the curves associated with the data are fits to a monomer-dimer-trimer equilibrium with freely varying dissociation constants (K_{12} and K_{13}). As described previously (Lear et al., 2001), the equilibrium distribution of peptide association states depends on the peptide/detergent ratio rather than the bulk peptide concentration. Thus, mole fraction units are used in the calculation of equilibrium constants and the appropriate standard state free energy of any component is that at unit mole fraction. In the bottom right panel, the minimum summed squared deviations of data points from fitted curves (χ^2) are plotted verses the negative logarithm of the dimer dissociation constant (pK_{12}) for fitting with fixed pK_{12} and variable pK_{13}. As the amount of dimer forced to be present in the model increases, the fit worsens. A maximum of ~10-20% dimer can be accommodated in the fitting model without a significant deterioration of the fit (increase in χ^2). The optimum fit (shown in Fig. 2) is when pK_{12} is 1.90 and pK_{13} is 5.01. The corresponding species plot (*bottom left panel*) shows a maximum dimer fraction of 12%. A similar treatment (not shown) of our previous AUC data (Choma et al., 2000) taken in 4 mM C14-betaine, gave $pK_{12} = 2.1$ and $pK_{13} = 4.9$, within experimental uncertainty of the values found in this work. At 40°C, data at both pH 4 and pH 7 (not shown) could be fit well with a monomer-dimer-trimer model predicting nearly the same distribution of dimer and trimer as that observed at 25°C.

With DPC in place of C14-betaine, however, analysis of AUC data showed the proportion of dimer to be much

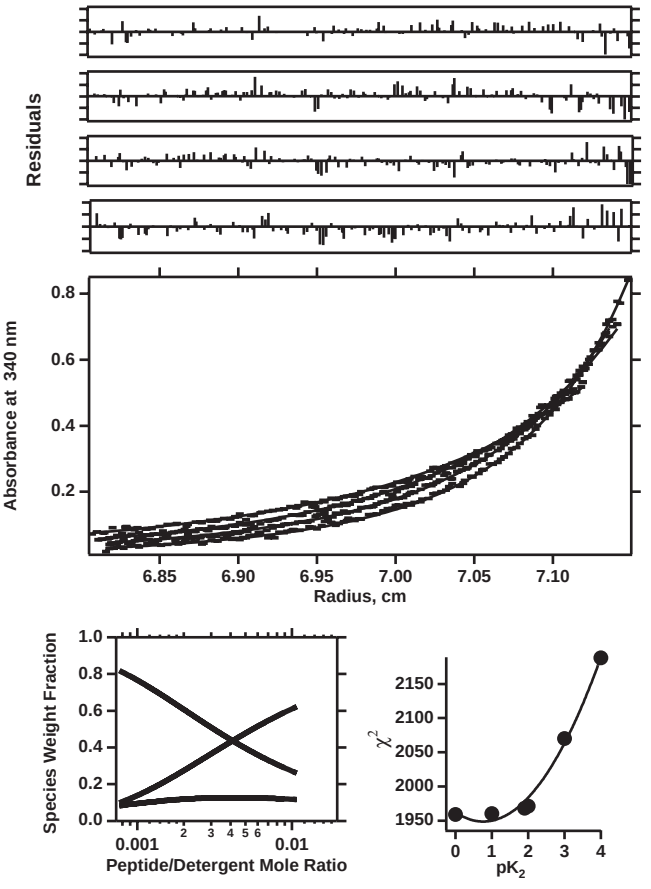

FIGURE 2 Equilibrium analytical ultracentrifugation results for the MS1 peptide in 8 mM C14-betaine micelles. The top four panels show the residuals of a monomer-trimer model fitted to data obtained at 40, 50, 55, and 60 KRPM, respectively. Full scale for each panel is ± 0.02 absorbance units. Data and fitted curves are shown in the middle panel. Bottom panels summarize results of fitting to a monomer-dimer-trimer model, fixing the dimer pK to values of 0, 1, 2, 3, and 4, and allowing the trimer pK to adjust to minimize the sum of squared deviations between calculated and measured data points. Data were weighted by the standard error of the individual absorbance measurements. Minimum squared deviations from the weighted curve fit (χ^2) are plotted against the fixed values of the dimer pK in the right panel. The left panel shows monomer, dimer, and trimer weight fractions for optimum fit values of pK_2 (1.90) and pK_3 (5.01).

greater, regardless of temperature or pH. For example, in Fig. 3, the sedimentation equilibrium experiment from MS1 in 10 mM DPC at pH 7 and 25°C is shown along with the curves that best fit the data. In the bottom left panel the species plot clearly shows that there is always a considerable amount of dimer present throughout a large range of peptide/detergent mole ratios. Only at extreme peptide/detergent mole ratios does the trimer predominate. In the graph in the bottom right panel, the χ^2 values from the curve fits are plotted against different fixed pK values for the dimer. The best pK_{12} is 3.45 with a well-defined optimum, unlike that observed in C14-betaine.

Sedimentation equilibrium experiments were performed at pH 4 and pH 7 and at 25°C and 40°C in both DPC and

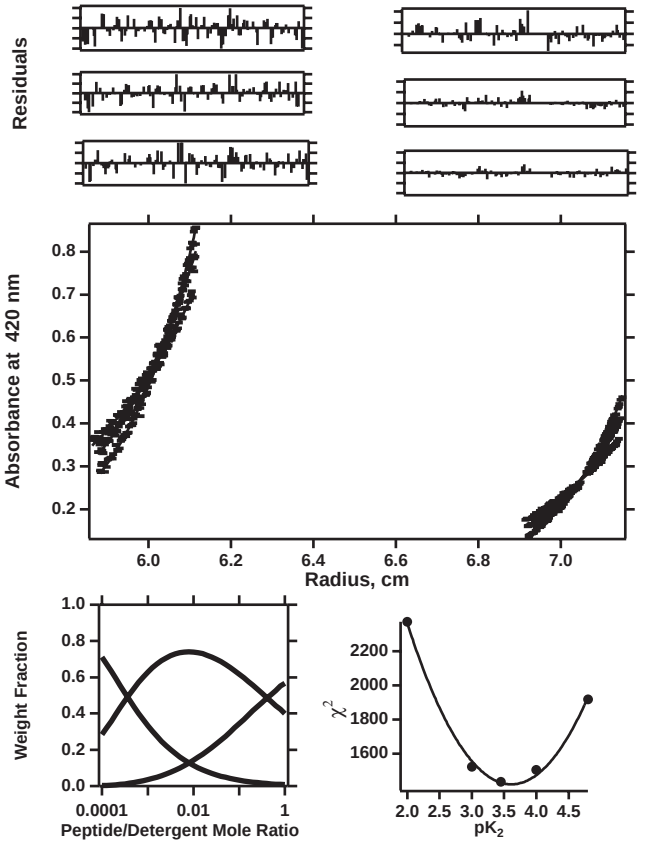

FIGURE 3 Equilibrium analytical ultracentrifugation results for MS1 peptide in 10 mM DPC micelles at 25°C. Top panels show residuals of monomer-dimer-trimer model curve-fit to data at, respectively, 40, 45, and 48 KRPM. Full scale for each panel is ± 0.02 absorbance units. Data and fitted curves are shown in the middle panel. The bottom right panel summarizes results of fitting to a monomer-dimer-trimer model, fixing the dimer pK to values of 0, 1, 2, 3, and 4, and allowing the trimer pK to adjust to minimize the sum of squared deviations between calculated and measured data points. Data were weighted by the standard error of the individual absorbance measurements. Minimum squared deviations from the weighted curve fit (χ^2) are plotted against the fixed values of the dimer pK. The left panel shows monomer, dimer, and trimer weight fractions for optimum fit values of pK_2 (3.45) and pK_3 (5.5) where both parameters were allowed to vary together in the curve-fitting.

C14-betaine detergents to allow a reliable comparison with NMR experiments (see below), which were done at 40°C and pH 4 for better resolution. Expressing the equilibria as monomer-dimer (K_{12}) and dimer-trimer ($K_{23} = K_{13}/K_{12}$) reactions (to maintain the dimensionality of the units), the pK values and corresponding free energy differences between monomer and dimer and dimer and trimer (ΔG_{12}, ΔG_{23}, unit mole fraction standard states) derived from the AU experiments are summarized in Table 1.

TABLE 1 Values of pK_{12} and pK_{23} (= $pK_{13} - pK_{12}$) derived from curve-fitting of AU data for MS1 at the noted conditions using a monomer-dimer-trimer equilibrium model with freely varying equilibrium constants

Detergent, Temp, pH	pK_{12}	pK_{23}	ΔG_{12} (kcal/mol.)	ΔG_{23} (kcal/mol)
C14-betaine				
25°C pH 7	1.9 ± 0.2	3.2 ± 0.3	2.6 ± 0.4	4.4 ± 0.5
40°C pH 7	1.9 ± 1	2.4 ± 1	2.6 ± 2	3.3 ± 2
40°C pH 4	2.3 ± 0.2	2.6 ± 0.2	3.1 ± 0.4	3.4 ± 0.4
DPC				
25°C pH 7	3.4 ± 0.1	2.1 ± 0.1	4.6 ± 0.2	2.8 ± 0.2
40°C pH 7	2.5 ± 0.2	2.8 ± 0.2	3.4 ± 0.4	3.8 ± 0.4
40°C pH 4	2.7 ± 0.5	1.9 ± 0.7	3.7 ± 0.7	2.6 ± 1

Corresponding ΔG values (kcal/mol) are calculated for a unit mole fraction standard state from $\Delta G_{ij} = 2.303\ RT\ pK_{ij}$. Error ranges shown are rounded-upward estimates from those computed by the curve-fitting algorithm. pK_{12} and pK_{13} errors were summed to compute error in pK_{23}.

NMR spectroscopy

NMR was utilized to more accurately determine the cooperativity of MS1 trimerization. In particular, Asn-14, which is essential to the oligomerization of MS1, was isotopically labeled with ^{15}N at the backbone and side chain nitrogen. To enhance the sensitivity by decreasing the effective correlation time of the peptide/detergent complex, experiments were performed at pH 4 and at 40°C. ^{15}N-HSQC spectra were collected at peptide/detergent mole ratios of 1/1750, 1/500, 1/225, and 1/125 (Fig. 4). The volumetric peptide

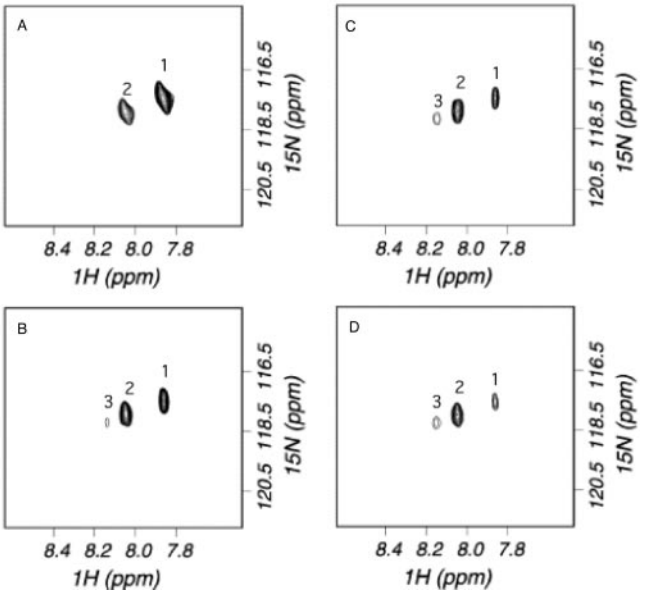

FIGURE 4 NMR 2D ^{15}N-HSQC spectra at different peptide/detergent ratios. ^{15}N Asn MS1 was at a concentration of 200 μM and deuterated DPC concentrations varied based on the molar peptide/detergent ratios. Peaks are labeled as follows: 1 represents the peak corresponding to the monomeric species, 2 represents the peak corresponding to the dimeric species, and 3 represents the peak corresponding to the trimeric species. In *a* the molar ratio is 1/1750, *b* is 1/500, *c* is 1/225, and *d* is 1/125. As the amount of detergent decreases, peaks assigned to the dimer and trimer grow, while that of the monomer diminishes. Data were collected at 40°C in 100 mM sodium phosphate, pH 4.0.

concentration remained the same while that of the deuterated DPC varied. A chemical shift change is observed between the Asn backbone peaks from the three different species. The chemical environment of the ^{15}N in the backbone differs enough among monomer, dimer, and trimer for a resonance corresponding to each oligomeric state to be observed. The side chain labels are not observed presumably because the amide hydrogens are converting between different H-bounded conformers on a time scale precluding their observation by NMR (Junius et al., 1995). Indeed, in deuterated methanol, where the peptide is monomeric (data not shown) the labeled peptide shows one peak for the backbone ^{15}N along with the two signature side chain peaks (Wuthrich, 1986).

Table 2 summarizes the relative values of the integrated HSQC signal peaks shown in Fig. 4. When integrated, it is found that the two large peaks observed at 1/1750 of MS1/DPC have relative intensities of 70% and 30%. Based on the centrifuge data in DPC at 25°C, the larger fraction is assigned to the monomeric species. As the amount of detergent is decreased, a third peak begins to appear and grows, but the intensity of this third peak only reaches 27% at a peptide/detergent ratio of 1/125. Because three peaks are present, the second peak, which is initially present in the 1/1750 peptide/detergent spectrum, is assigned to the dimeric population and the final peak that appears is assigned to the peptides participating in a trimeric association. The peak corresponding to monomer decreases as the amount of detergent decreases, whereas there is always a considerable amount of dimer present throughout the range of concentrations examined. The NMR data thus suggest that MS1 is a very weakly cooperative system in DPC at pH 4 and 40°C.

This conclusion was confirmed by AU measurements in DPC at pH 4 and 40°C in DPC. Importantly, the species distribution deduced from the NMR data (data points in Fig. 5) was essentially the same as that predicted from the sedimentation equilibrium data (*lines*). Dimer is continuously present, and the trimer remains a minor component over the peptide/detergent molar ratios experimentally used.

DISCUSSION

Because the cooperativity of MS1 trimerization was uncertain, we obtained AUC data for MS1 at different speeds, temperatures, pH values, and peptide/detergent mole ratios in two different, density-matched detergents (C14-betaine and DPC), and we analyzed the data using a reversible monomer-dimer-trimer equilibrium model. Moreover, we used NMR measurements in a detergent (DPC) available in perdeuterated form to confirm the AUC results. The MS1 trimerization exhibits different cooperativity in different detergents. In SDS micelles, we previously observed only a single trimeric species by SDS-PAGE. Similarly, in C14-betaine micelles, though a cooperative monomer-trimer equilibrium provided a satisfactory fit to the AUC data, a slightly better fit was obtained with a monomer-dimer-trimer equilibrium. This result was confirmed and made more quantitative in this study; in C14 betaine, no more than 20% of the dimer intermediate occurs in the overall monomer-trimer equilibrium of MS1. However, in DPC micelles, the dimer intermediate is highly populated at the midpoint of the MS1 monomer-trimer equilibrium. Thus, the specificity of MS1 for forming trimers over other aggregation states is not absolute, and changes of detergent type can affect the free energy level of the trimer relative to the dimer.

The packing of MS1 was initially modeled after the core of GCN4-P1 (Choma et al., 2000), a well-packed, coiled-coil dimer (O'Shea et al., 1991). Hydrophobic residues at "a" and "d" positions in the heptad repeat drive the association and give stability to the native structure. By altering which hydrophobic side chain resides at an "a" position and/or a "d" position, a variety of association states can be specified (Betz et al., 1995; Harbury et al., 1993). With Val at "a" positions and Leu at "d" positions, the water-soluble GCN4-P1 peptide forms both dimers and trimers, indicating that the side chain packing required for each state is favorable. Therefore, in the MS1 system where the asparagine stabilizes, rather than destabilizes the association, it is reasonable to expect a mixture of aggregation states.

An important goal of these studies was to establish a firm basis for quantitative calculations of free energies of helix association in model membrane systems. Free energy differences between systems exhibiting three-state equilibria can come from differences in one or all equilibrium states. The difference in free energy, $\Delta G_{23} - \Delta G_{12}$, for MS1 at 25°C, pH 7 in Table 1 is + 1.8 kcal/mol for C14-betaine and −1.8 for DPC. Although such a small energetic difference would require only very subtle changes in structure, it is nevertheless large enough to cause measurable differences in cooperativity. Comparing the two detergents' chemical structures (Fig. 1), it is interesting that the charges on the zwitterionic headgroups have opposite spatial distributions. We can speculate that this difference might be reflected in solvation differences among the various species. Whatever the reasons, this result emphasizes that small differences in the membrane environment of membrane proteins can modulate the structural features and, by inference, the function of membrane proteins. Indeed, the function of reconstituted native membrane proteins can be profoundly affected by the choice of detergents and lipids used for solubilization (e.g., Epstein and Racker, 1978).

These results can be compared with those reported for designed coiled-coil peptides showing a monomer-dimer-trimer equilibrium in aqueous systems (Betz et al., 1995). A series of peptides in which the core "a" and "d" positions are all occupied by leucine showed an average $\Delta G_{23} - \Delta G_{12} = -1.8$, the same as observed for MS1 in DPC. Interestingly, the pK_{12} values in the aqueous system, calcu-

TABLE 2 Percentage of monomer, dimer, and trimer peak areas at different peptide/detergent mole ratios. HSQC peaks were integrated in Felix98

Peptide/ Detergent Mole Ratio	Peak 1 (%) Monomer	Peak 2 (%) Dimer	Peak 3 (%) Trimer
1/1750	68.6	31.4	0
1/500	45.3	47.1	7.6
1/225	26.3	57.4	16.3
1/125	18.4	55.0	26.6

lated for a unit mole fraction standard state (by addition of 2.3 RT log55) and in the absence of denaturant, are about six to seven units (~9 kcal/mol) greater than those for the MS1 system, indicating a much tighter association, most likely driven by the hydrophobic effect.

Although our measurements at different temperatures were not intended to determine enthalpies of association, the van't Hoff enthalpy calculated for the MS1 dimer-trimer equilibrium at pH 7 in DPC at 25° versus 40°C (the largest observed difference) is 25 kcal/mol. This value, a calculated upper limit, is still significantly smaller than that of GCN4 (~35 kcal/mol, Thompson et al., 1993). This is consistent with the fact that because MS1 is confined to the detergent phase, its secondary structure is largely independent of aggregation, whereas the GCN4 dimer undergoes a helix-coil transition upon dissociation in water, losing the enthalpy of helix formation (0.9–1.3 kcal/mol-residue, see Wieprecht et al., 1999).

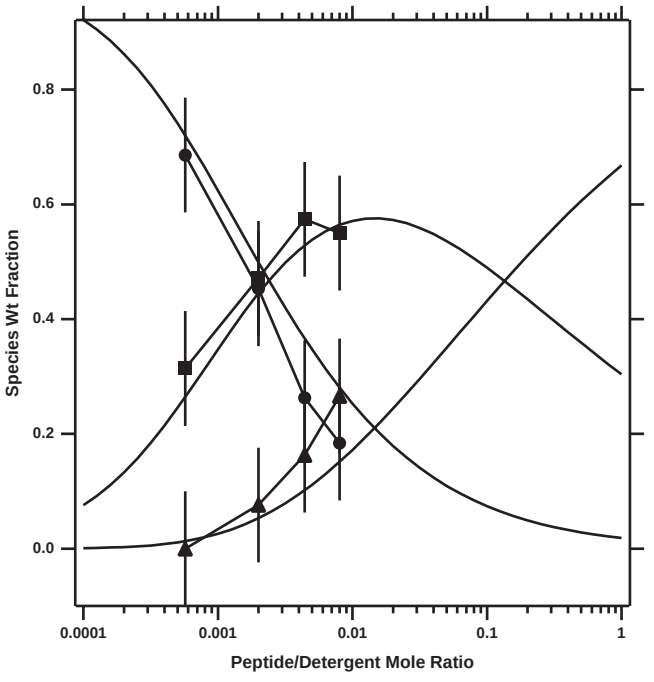

FIGURE 5 Species plot comparing results from NMR and sedimentation equilibrium data for the MS1 peptide. Sedimentation equilibrium experiments were performed at pH 4.0 in 100 mM sodium phosphate buffer, 10 mM DPC, and at 40°C to allow direct comparison to the NMR experiment. 38% D_2O was required to match buffer and detergent densities under these conditions. A monomer-dimer-trimer equilibrium model was used to globally fit data collected at 40 and 45 KRPM and at 0.0033 and 0.0067 mole fractions, allowing both pK values to vary freely. The weight fractions of monomer, dimer, and trimer computed from the fit parameters (pK_2 = 2.66, pK_3 = 4.55) are shown (*solid lines*) as a function of peptide/detergent mole ratio. Circles, squares, and triangles represent, respectively, the fractions of monomer, dimer, and trimer determined from integration of the HSQC peaks at the four different peptide/detergent mole ratios.

Previously (Gratkowski et al., 2001), we reported $\Delta\Delta G$ values (on a per-helix basis) for trimerization in C14-betaine of a number of MS1 mutants. Because many of the mutants associated so weakly that precise determination of the individual equilibria was not possible, $\Delta\Delta G$ values were computed for an assumed two-state, monomer-trimer equilibrium. In light of the findings here, those values were recalculated by refitting the AUC data using a monomer-dimer equilibrium that, because of the low degree of association, gives equally good fits. The results (not shown) are within the experimental error of those calculated previously, although the recalculated $\Delta\Delta G$ values are slightly larger.

In conclusion, we have demonstrated that the MS1 peptide forms both dimers and trimers in detergent micelles at the peptide/detergent ratios used in this and previous studies. The relative stability of the dimer versus the monomer is ~2 kcal/mol greater in DPC than in C14-betaine, but addition of another monomer to make a trimer is less favorable in DPC by ~1 kcal/mol. The association of MS1 in both detergents is weaker than that observed for similar peptides in water, and consistent with it being driven primarily by H-bonding interactions rather than by solvophobic effects. Our results demonstrate that analytical ultracentrifugation in conjunction with independent methods (in this case NMR) can be used to characterize multi-state equilibrium systems in detergents and hence can be applied to thermodynamic comparisons of these model peptides.

This work was supported by National Institutes of Health Grants GM60610 (to J.D.L.), GM35940 (to A,J.W.), and National Science Foundation Grant DMROD-79909 (to W.F.D. and in A.J.W.).

REFERENCES

Arkin, I. T., P. D. Adams, A. T. Brunger, S. Aimoto, D. M. Engelman, and S. O. Smith. 1997. Structure of the transmembrane cysteine residues in phospholamban. *J. Membr. Biol.* 155:199–206.

Arkin, M, and J. D. Lear. 2001. A new data analysis method to determine binding constants of small molecules to proteins using equilibrium analytical ultracentrifugation with absorption optics. *Anal. Biochem.* 299:98–107.

Betz, S., R. Fairman, K. O'Neil, J. Lear, and W. Degrado. 1995. Design of two-stranded and three-stranded coiled-coil peptides. *Phil. Trans. R. Soc. Lond. B. Biol. Sci.* 348:81–88.

Boice, J. A., G. R. Dieckmann, W. F. DeGrado, and R. Fairman. 1996. Thermodynamic analysis of a designed three-stranded coiled coil. *Biochemistry*. 359:14480–14485.

Chen, G. Q., and E. Gouaux. 1999. Probing the folding and unfolding of wild-type and mutant forms of bacteriorhodopsin in micellar solutions: evaluation of reversible unfolding conditions. *Biochemistry*. 389: 15380–15387.

Choma, C., H. Gratkowski, J. D. Lear, and W. F. DeGrado. 2000. Asparagine-mediated self-association of a model transmembrane helix. *Nat. Struct. Biol.* 7:161–166.

Cornea, R. L., L. R. Jones, J. M. Autry, and D. D. Thomas. 1997. Mutation and phosphorylation change the oligomeric structure of phospholamban in lipid bilayers. *Biochemistry*. 36:2960–2967.

Epstein, M., and E. Racker. 1978. Reconstitution of carbamylcholine-dependent sodium ion flux and desensitization of the acetylcholine receptor from *Torpedo californica*. *J. Biol. Chem.* 253:6660–6662.

Fisher, L. E., D. M. Engelman, and J. N. Sturgis. 1999. Detergents modulate dimerization but not helicity, of the glycophorin A transmembrane domain. *J. Mol. Biol.* 293:639–651.

Fleming, K. G., A. L. Ackerman, and D. M. Engelman. 1997. The effect of point mutations on the free energy of transmembrane alpha-helix dimerization. *J. Mol. Biol.* 272:266–275.

Fleming, K. G., and D. M. Engelman. 2001. Specificity in transmembrane helix-helix interactions can define a hierarchy of stability for sequence variants. *Proc. Natl. Acad. Sci. U. S. A.* 98:14340–14344.

Friedrichs, M. S., L. Mueller, and M. Wittekind. 1994. An automated procedure for the assignment of protein 1HN, 15N, 113Ca, 1Ha, 13Cb and 1Hb resonances. *J. Biomol. NMR*, 4:703–726.

Garavito, R. M., and S. Ferguson-Miller. 2001. Detergents as tools in membrane biochemistry. *J. Biol. Chem.* 276:32403–32406.

Gonzalez, L, Jr., R. A. Brown, D. Richardson, and T. Alber. 1996a. Crystal structures of a single coiled-coil peptide in two oligomeric states reveal the basis for structural polymorphism. *Nat. Struct. Biol.* 3:1002–1009.

Gonzalez, L, Jr., J. J. Plecs, and T. Alber. 1996b. An engineered allosteric switch in leucine-zipper oligomerization. *Nat. Struct. Biol.* 3:510–515.

Gonzalez, L, Jr., D. N. Woolfson, and T. Alber. 1996c. Buried polar residues and structural specificity in the GCN4 leucine zipper. *Nat. Struct. Biol.* 3:1011–1018.

Gratkowski, H., J. D. Lear, and W. F. DeGrado. 2001. Polar side chains drive the association of model transmembrane peptides. *Proc. Natl. Acad. Sci. U.S.A.* 98:880–885.

Harbury, P. B., T. Zhang, P. S. Kim, and T. Alber. 1993. A switch between two-, three-, and four-stranded coiled coils in GCN4 leucine zipper mutants. *Science*. 262:1401–1407.

Junius, F. K., J. P. Mackay, W. A. Bubb, S. A. Jensen, A. S. Weiss, and G. F. King. 1995. Nuclear magnetic resonance characterization of the Jun leucine zipper domain: unusual properties of coiled-coil interfacial polar residues. *Biochemistry*. 34:6164–6174.

Kharakoz, D. P. 1997. Partial volumes and compressibilities of extended polypeptide chains in aqueous solution: additivity scheme and implication of protein unfolding at normal and high pressure. *Biochemistry*. 36:10276–10285.

Kochendoerfer, G. G., D. Salom, J. D. Lear, R. Wilk-Orescan, S. B. Kent, and W. F. DeGrado. 1999. Total chemical synthesis of the integral membrane protein influenza A virus M2: role of its C-terminal domain in tetramer assembly. *Biochemistry*. 38:11905–11913.

Laue, T., B. D. Shaw, T. M. Ridgeway, and S. L. Pelletier. 1992. Computer-aided interpretation of analytical sedimentation data for proteins. S. E. Harding, A. J. Rowe, and J. C. Horton, editors. The Royal Society of Chemistry, Cambridge, U.K. 90–125.

Lear, J. D., H. Gratkowski, and W. F. Degrado. 2001. De novo design, synthesis and characterization of membrane-active peptides. *Biochem. Soc. Trans.* 29:559–564.

Lemmon, M. A., J. M. Flanagan J. F. Hunt, B. D. Adair, B-J. Bormann, C. E. Dempsey, and D. M. Engelman. 1991. Glycophorin A dimerization is driven by specific interactions between transmembrane alpha-helices. *J. Biol. Chem.* 267:7683–7689.

Li, M., L. G. Reddy, R. Bennett, N. D. Jr., Silva, L. R. Jones, and D. D. Thomas. 1999. A fluorescence energy transfer method for analyzing protein oligomeric structure: application to phospholamban. *Biophys. J.* 76:2587–2599.

O'Shea, E. K., J. D. Klemm, P. S. Kim, and T. Alber. 1991. X-ray structure of the GCN4 leucine zipper, a two-stranded, parallel coiled coil. *Science*. 254:539–544.

Sakaguchi, T., T. Qiang, L. H. Pinto, and R. A. Lamb. 1997. The active oligomeric state of the minimalist influenza virus M2 ion channel is a tetramer. *Proc. Natl. Acad. Sci. U.S.A.* 94:5000–5005.

Salom, D., B. R. Hill, J. D. Lear, and W. F. DeGrado. 2000. pH-dependent tetramerization and amantadine binding of the transmembrane helix of M2 from the influenza A virus. *Biochemistry*. 39:14160–14170.

Scott, C. P., O. B. Kashlan, J. D. Lear, and B. S. Cooperman. 2001. A quantitative model for allosteric control of purine reduction by murine ribonucleotide reductase. *Biochemistry*. 40:1651–1661.

Tanford, C., and J. A. Reynolds. 1976. Characterizattion of membrane proteins in detergent solutions. *Biochim. Biophys. Acta*. 457:133–170.

Thompson, K. S., C. R. Vinson, and E. Freire. 1993. Thermodynamic characterization of the structural stability of the coiled-coil region of the bZIP transcription factor GCN4. *Biochemistry*. 32:5491–5496.

Wieprecht, T., O. Apostoloy, M. Beyermann, and J. Seelig. 1999. Thermodynamics of the alpha-helix-coil transition of amphipathic peptides in a membrane environment: implications for the peptide-membrane binding equilibrium. *J. Mol. Biol.* 294:785–794.

Wuthrich, K. 1986. NMR of Proteins and Nucleic Acids. Wiley, New York.

Zhou, F. X., M. J. Cocco, W. P. Russ, A. T. Brunger, and D. M. Engelman. 2000. Interhelical hydrogen bonding drives strong interactions in membrane proteins. *Nat. Struct. Biol.* 7:154–160.

Zhou, Y., F. W. Lau, S. Nauli, D. Yang, and J. U. Bowie. 2001. Inactivation mechanism of the membrane protein diacylglycerol kinase in detergent solution. *Protein Sci.* 10:378–383.